Impact of new land boundary conditions from Moderate Resolution Imaging Spectroradiometer (MODIS) data on the climatology of land surface variables

Y. Tian, R. E. Dickinson, L. Zhou, and M. Shaikh

School of Earth and Atmospheric Sciences, Georgia Institute of Technology, Atlanta, Georgia, USA

Received 30 December 2003; revised 14 July 2004; accepted 22 July 2004; published 28 October 2004.

[1] This paper uses the Community Land Model (CLM2) to investigate the improvements of a new land surface data set, created from multiple high-quality collection 4 Moderate Resolution Imaging Spectroradiometer data of leaf area index (LAI), plant functional type, and vegetation continuous fields, for modeled land surface variables. The previous land surface data in CLM2 underestimate LAI and overestimate the percent cover of grass/crop over most of the global area. For snow-covered regions with abundant solar energy the increased LAI and percent cover of tree/shrub in the new data set decreases the percent cover of surface snow and increases net radiation and thus increases ground and surface (2-m) air temperature, which reduces most of the model cold bias. For snow-free regions the increased LAI and changes in the percent cover from grass/crop to tree or shrub decrease ground and surface air temperature by converting most of the increased net radiation to latent heat flux, which decreases the model warm bias. Furthermore, the new data set greatly decreases ground evaporation and increases canopy evapotranspiration over tropical forests, especially during the wet season, owing to the higher LAI and more trees in the new data set. It makes the simulated ground evaporation and canopy evapotranspiration closer to reality and also reduces the warm biases over tropical regions. *INDEX TERMS:* 1620 Global Change: Climate dynamics (3309); 1640 Global Change: Remote sensing; 3307 Meteorology and Atmospheric Dynamics: Boundary layer processes; 3322 Meteorology and Atmospheric Dynamics: Land/atmosphere interactions; *KEYWORDS:* MODIS, Community Land Model, land surface data, land surface variables

Citation: Tian, Y., R. E. Dickinson, L. Zhou, and M. Shaikh (2004), Impact of new land boundary conditions from Moderate Resolution Imaging Spectroradiometer (MODIS) data on the climatology of land surface variables, *J. Geophys. Res.*, *109*, D20115, doi:10.1029/2003JD004499.

1. Introduction

[2] The land component of climate models represents many important processes that control the transfers of water and energy to the atmosphere. The absorption of solar energy is a dominant process that is related to surface properties such as land cover type, leaf area index (LAI), and fractional vegetation cover (FVC) [*Zeng et al.*, 2000]. Several climate model simulations have shown significant sensitivities to these land surface characteristics. *Chase et al.* [1996] found that decreasing LAI globally decreased surface latent heat flux and increased sensible heat flux during January and July in general circulation model simulations. *Bonan* [1997] showed that the land-use change of natural vegetation to present-day vegetation cover caused a cooling of 1 K in the eastern United States and a warming of 1 K in the western United States during spring and a cooling of ~2 K during summer over large regions of the central United States. Studies by *Xue et al.* [1996] and *Lu and Shuttleworth* [2002] found that vegetation phenology and land surface heterogeneity associated with vegetation cover could have a significant influence on predictions of surface temperature and precipitation. Thus both the spatial and temporal distribution of vegetation in climate models is needed in some detail.

[3] The importance of remotely sensed data of the land surface has been demonstrated in land models [*Buermann et al.*, 2001; *Oleson and Bonan*, 2000; *Oleson et al.*, 2000; *Lu and Shuttleworth*, 2002; *Bonan et al.*, 2002a, 2002b; *Zeng et al.*, 2002]. Discrepancies from observations in surface variables such as albedo, fraction of photosynthetically active radiation (0.4–0.7 μm) absorbed by vegetation, and surface temperature have been identified in the Community Land Model (CLM2) [*Bonan et al.*, 2002a], Common Land Model [*Zeng et al.*, 2002], and Land Surface Model [*Bonan*, 1998] when these models were evaluated in the context of observations and a common atmosphere model [*Bonan et al.*, 2002a; *Oleson et al.*, 2003; *Tian et al.*, 2004a; *Zhou et al.*, 2003a, 2003b]. These biases were attributed either to inaccurate specification of land surface parameters such as

0148-0227/04/2003JD004499$09.00

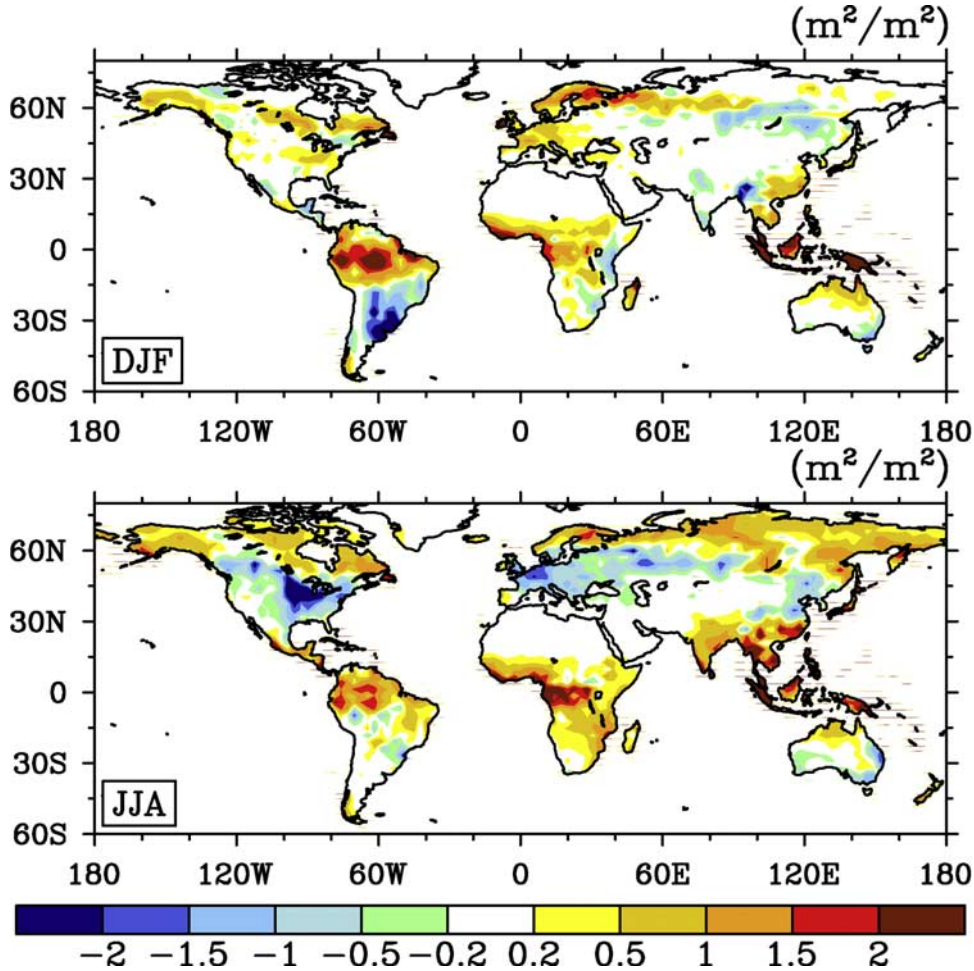

Figure 1. Spatial pattern of LAI difference between the new and old land surface data sets (new minus old) in winter (DJF) and summer (JJA).

LAI, stem area index, leaf optical properties, and soil albedo or to unrealistic treatments of snow albedo related variables such as snow cover, snow age, and solar zenith angle dependence of snow albedo.

[4] Changes in LAI over vegetated land surfaces can directly influence a climate model's surface albedo, canopy conductance, and plant evapotranspiration, and thus net solar radiation [*Buermann et al.*, 2001]. Climate simulations also depend on the accuracy of specification of land cover types. Vegetation types differ in their parameters such as LAI, albedo, vegetation root distribution, roughness length, and stomatal resistance [*Bonan*, 1996]. Forests generally have higher LAI, lower albedo, deeper roots, and higher roughness length than grasses or shrubs, and thus they have higher canopy evapotranspiration and lower temperature. FVC indicates the horizontal heterogeneity of vegetation. Its inaccurate specification from lack of data could result in errors in albedo and hence in energy balance even with the LAI specified precisely. Evidently, use of inaccurate or incorrect land surface data in climate models could result in large biases in regional and global climate simulations by causing a misrepresentation of the partitioning of available energy between sensible and latent heat and of precipitation between evapotranspiration and runoff [*Zhao et al.*, 2001].

[5] Do some of the model biases reported in the recent CLM2 studies result from inaccurate or inconsistent land surface data sets? Most of the land surface data sets currently used in climate models were derived from advanced very high resolution radiometers (AVHRRs), whose quality is degraded by atmospheric effects, satellite drift and changeover [*Gutman*, 1999]. For example, the current CLM2 uses an LAI data set, which was derived from only 1 year of AVHRR data (April 1992 to March 1993) based on a simple normalized difference vegetation index–LAI relationship, and a plant functional type (PFT) data set, which was derived without access to consistent FVC data and so assumed too much grasses, shrubs, or crops over the non-tree-covered land [*Bonan et al.*, 2002b; *Tian et al.*, 2004b].

[6] The recent availability of multiple high-quality Moderate Resolution Imaging Spectroradiometer (MODIS) land data makes it possible to investigate the global and regional effects of a new land surface data set on land surface variables in CLM2. This new data set has been derived from MODIS data of LAI, PFT, and FVC that is created from the MODIS vegetation continuous fields product [*Tian et al.*, 2004b]. Section 2 describes the data and methods. Sections 3

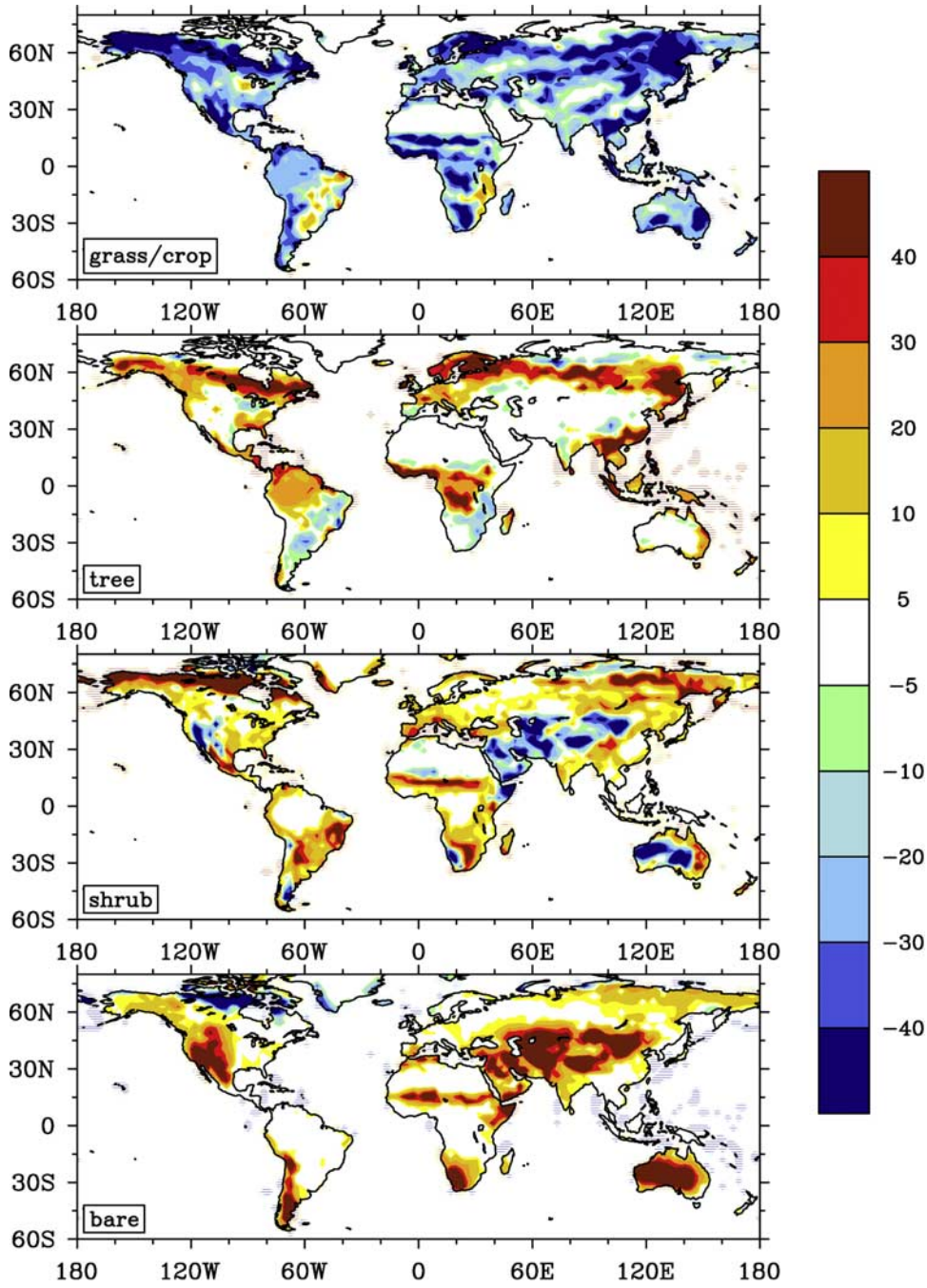

Figure 2. Spatial pattern of percent cover difference (new minus old) in grass/crop, tree, shrub, and bare soil at the model spatial resolution.

and 4 show how climate variables change globally and regionally after the new land surface data set is used, and section 5 finishes with discussion and conclusions.

2. Data and Methods

[7] Since MODIS includes seven spectral bands that are explicitly designed for land applications, the enhanced spectral, spatial, radiometric, and geometric quality of its data improves our capability for monitoring and mapping global land products such as LAI, land cover type, and vegetation continuous fields relative to AVHRR data [*Friedl et al.*, 2002; *Hansen et al.*, 2002; *Myneni et al.*, 2002]. To assess the biases of the AVHRR-derived land surface data set currently used in CLM2 (referred to as the old data hereinafter), we have created a new land surface data set from the latest MODIS LAI, vegetation continuous fields, International Geosphere-Biosphere Programme (IGBP) land cover map, and PFT map using procedures similar to those described by *Bonan et al.* [2002b]. First, we aggregate MODIS 500 m collection 3 Global Vegetation Continuous Fields [*DeFries et al.*, 1999], which contain percent of tree cover (tall trees), herbaceous cover (shrubs and grasses), and bare, from 2000 to 2001, to generate 1-km FVC data.

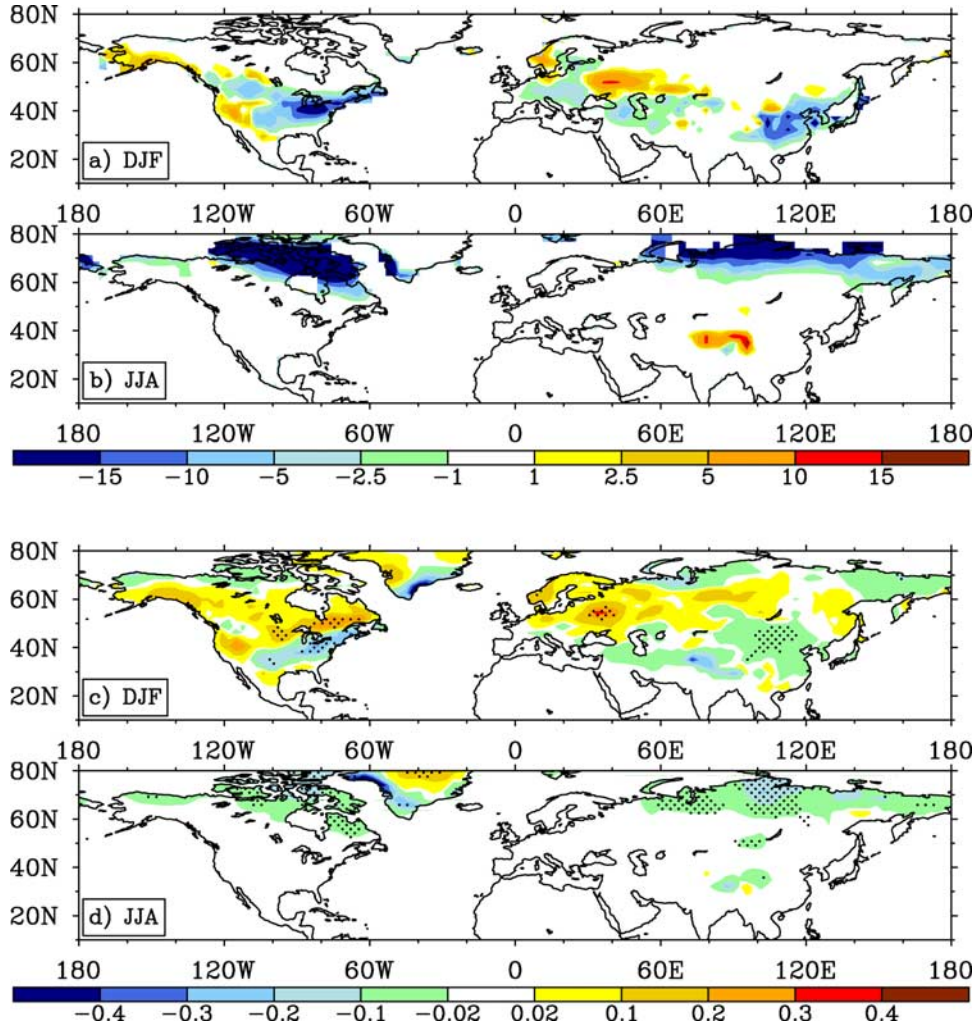

Figure 3. Spatial pattern of difference (experiment minus control) in percent cover of snow over ground for (a) winter and (b) summer and in solid precipitation (snow) for (c) winter and (d) summer. Stippling shows regions where the difference is statistically significant based on a *t* test ($p < 0.1$). The unit for solid precipitation is mm day^{-1}.

Second, we generate a 15-PFT data set at 0.5° resolution from the MODIS 1-km PFT and IGBP land cover maps. The MODIS PFT map consists of 7 primary PFTs and is expanded to 15 PFTs on the basis of climate rules [*Bonan et al.*, 2002b]. The 1-km data are aggregated to grid cells at 0.5° resolution by averaging the 1-km percentages per 0.5° grid cell, which normalized the percent of each grid cell covered by a particular PFT by the vegetated area [*Bonan et al.*, 2002b]. The bare ground in each grid cell is always considered to be the cumulative canopy opening. Third, we generate an LAI data set at 0.5° resolution from 2.5 years of collection 4 MODIS 1-km LAI data [*Myneni et al.*, 2002] with 8-day composite period. The MODIS 1-km data with the best quality are further composited to produce a climatology of monthly LAI and are then used to derive the seasonal course of LAI for every PFT at a 0.5° grid cell. Note that for each PFT a pure PFT LAI is estimated at a 0.5° grid cell by averaging only the LAIs over 1-km pixels whose abundance of the PFT is >60%. Finally, these three major data sets at 0.5° resolution are aggregated into the model grids for use in CLM2. Details about these procedures are given by *Tian et al.* [2004b]. The surface data for ocean, wetland, lake, and snow-ice land cover types are unchanged and not considered here.

[8] We performed two 21-year simulations of CLM2 coupled with the National Center for Atmospheric Research (NCAR) Community Atmosphere Model (CAM2) [*Blackmon et al.*, 2001] at ~2.8° resolution using observed sea surface temperature from January 1979 to December 1999 to examine changes in surface variables due to differences in the land surface data. For simplicity the simulation with the old data is referred to as the "control run" and that with the new data is referred to as the "experiment." All variable values from the last 20 years are used for comparison while the first 1-year run is used as a spin-up. Comparison of these two simulations demonstrates the major improvements contributed by the new data.

[9] A monthly climatology of land surface air (2-m) temperature from the National Centers for Environmental Prediction (NCEP)/NCAR reanalysis [*Kalnay et al.*, 1996; *Kistler et al.*, 2001] was compared with that from our simulations. The reanalysis uses the most extensive obser-

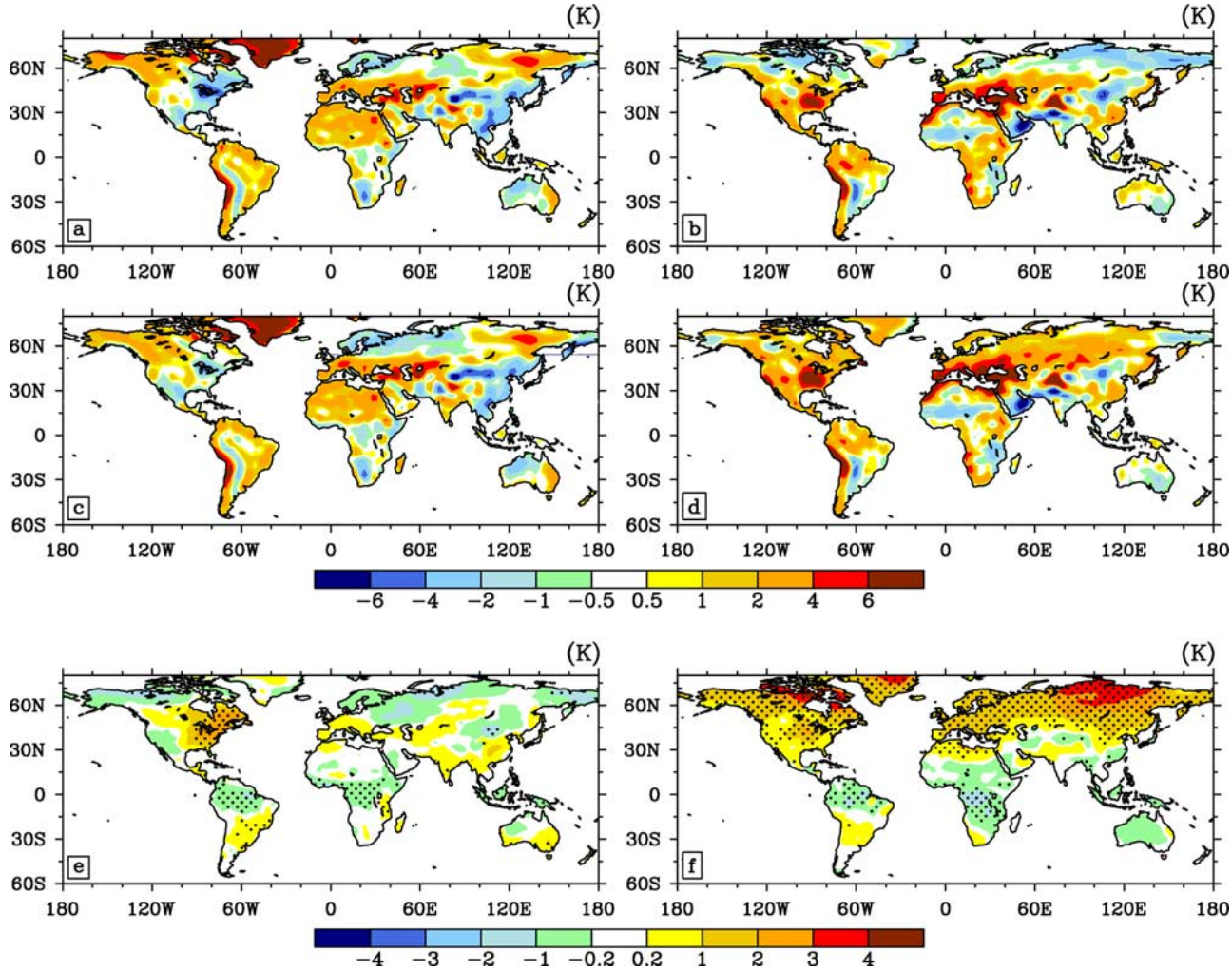

Figure 4. Surface air (2m) temperature difference between the control run and National Centers for Environmental Prediction (NCEP) data (control minus NCEP) for (a) winter and (b) summer, difference between the experiment run and NCEP data (experiment minus NCEP) for (c) winter and (d) summer, and difference between the experiment and control run (experiment minus control) for (e) winter and (f) summer. Surface air temperature in CLM2 is the average over all time steps. Stippling shows regions where the difference is statistically significant based on a t test ($p < 0.1$).

vations available from a variety of sources, including land station and ship observations, upper air rawinsonde measurements, pibal, aircraft, and satellite observations, etc., to assimilate these data from 1948 to the present on the basis of a state-of-the-art analysis/forecast system. It has a resolution at $\sim$1.8° on a Gaussian grid, with a total of 192 × 94 grid cells globally.

3. Spatial Patterns of Difference at Global Scales

3.1. Differences in the Land Surface Data

[10] Figure 1 shows differences in LAI for winter (DJF) and summer (JJA) between the new and old land surface data. The new LAI is larger than the old data by at least 1.5 over the Amazon, central Africa, southeastern Asia, and north Europe and by $\sim$0.5–1.0 over most areas beyond 60°N in both seasons. New values are smaller by $\sim$0.5–1.5 over extratropical South America in winter and over the eastern United States and middle latitude Eurasia (30°–60°) in summer.

[11] Figure 2 shows differences in the percent cover of grass/crop, tree, shrub, and bare soil between the new and old data. The percent cover of bare soil at each grid cell is defined as 1 minus total FVC (the sum of FVC for grass/crop, tree, and shrub). The old data overestimate the percent cover of grass/crop by $\sim$20–40% globally, especially over the belt 45°–70°N, and underestimate that of tree or shrub over most of the Amazon, central Africa, and the region in 45°–70°N. They also underestimate the percent cover of bare soil by putting too much shrub over sparsely vegetated areas such as the Sahel, Tibet, Australia, and the western United States. The latter two of them have especially low percent cover of bare soil (only about 0 $\sim$ 1%) in the old data. In contrast, the old data overestimate the percent cover of bare soil for shrubs in northeast Canada.

3.2. Differences in Percent Cover of Snow

[12] Figures 3a and 3b compare the percent cover of snow over ground (f_{sn}), defined as the fraction of ground covered

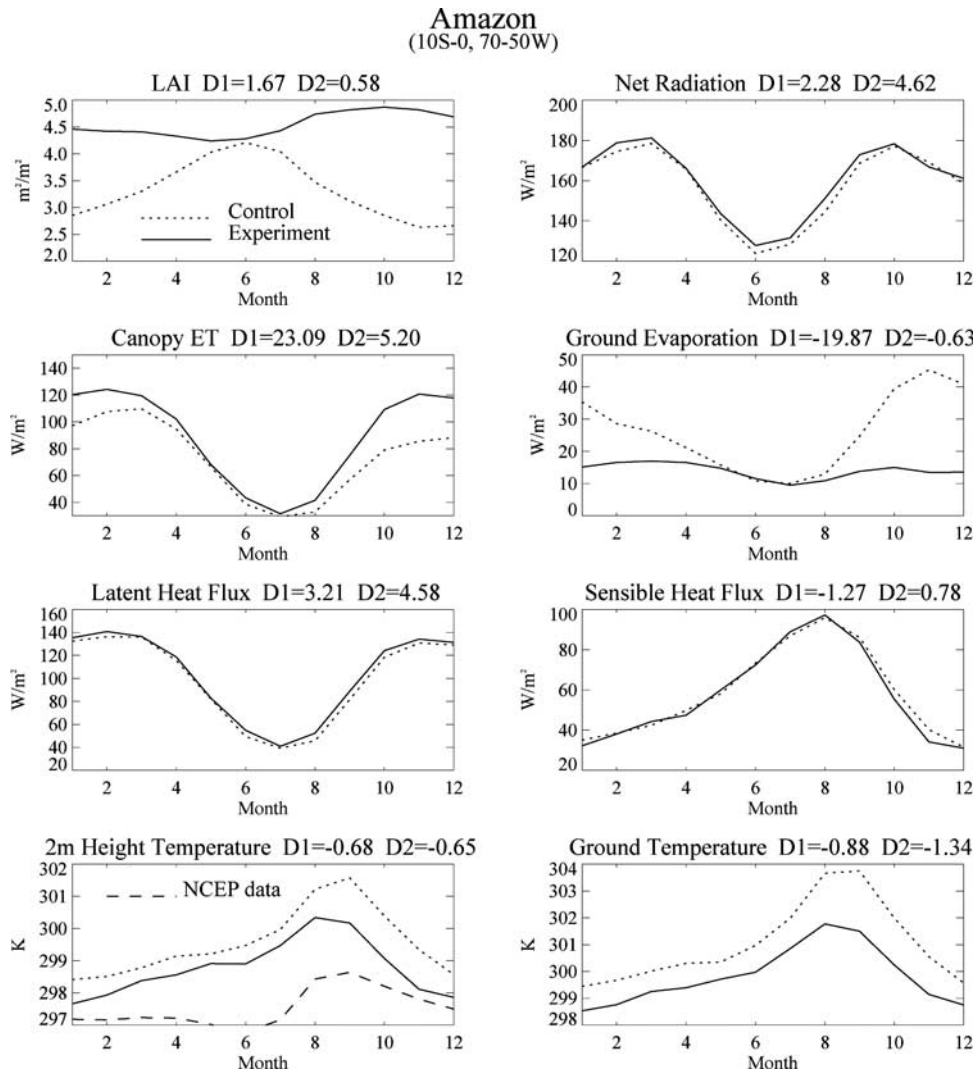

Figure 5. Regionally averaged monthly surface variables for the control run and experiment in Amazon. Note that net radiation equals absorbed solar radiation minus net longwave loss. The symbols of "D1" and "D2" represent the average difference (experiment minus control) for each variable in DJF and JJA, respectively.

by snow regardless whether it is beneath a canopy or over bare soil, between the experiment and control run. The grid cell value of f_{sn} is a weighted average of the percent cover of snow for four PFTs (one of which may be bare soil) where the weights are the relative areas of the four PFTs. If wetlands, glaciers, and/or lakes are present within the grid cell, their fractional snow has to be averaged in as well. Since the percent cover of snow could be affected by increases or decreases in solid precipitation (snow) due to changes in land surface data, its differences at global scales between the experiment and control run are shown in Figures 3c and 3d including a statistical test (e.g., Student's *t* test).

[13] In summer the new data decrease f_{sn} over northern high latitudes because of increased LAI and a significant decrease in solid precipitation. The winter value of f_{sn} increases over Tibet, mainly from the increase in the percent cover of bare soil because LAI, stem area index, and snow do not change too much between the two simulations over this region. It varies little beyond 50°N where 100% of the ground is covered by snow but changes with LAI and snow below 50°N. A decrease in f_{sn} corresponds to an increase in LAI and a significant decrease in snow over areas such as the eastern United States and southeast China, except in central Europe where only an increase in LAI contributes to a decrease in f_{sn}. In the western United States, f_{sn} increases because of the increased snow and percent cover of bare soil. Evidently, changes in the percent cover of snow are influenced not only directly by land surface changes such as LAI and percent cover of bare soil but also indirectly by feedbacks triggered by these land surface changes.

[14] *Tian et al.* [2004b] indicate that surface albedo from the experiment run over snow-covered surface is largely reduced in areas where LAI increases because such increase decreases albedo and f_{sn}, which, in turn, also decreases albedo. Over snow-free regions, albedos are lower mainly because of the reduction of percent cover of grass/crop because grass/crop has significantly higher albedo than other PFTs (more significantly in the near infrared than visible) [*Oleson and Bonan*, 2000;

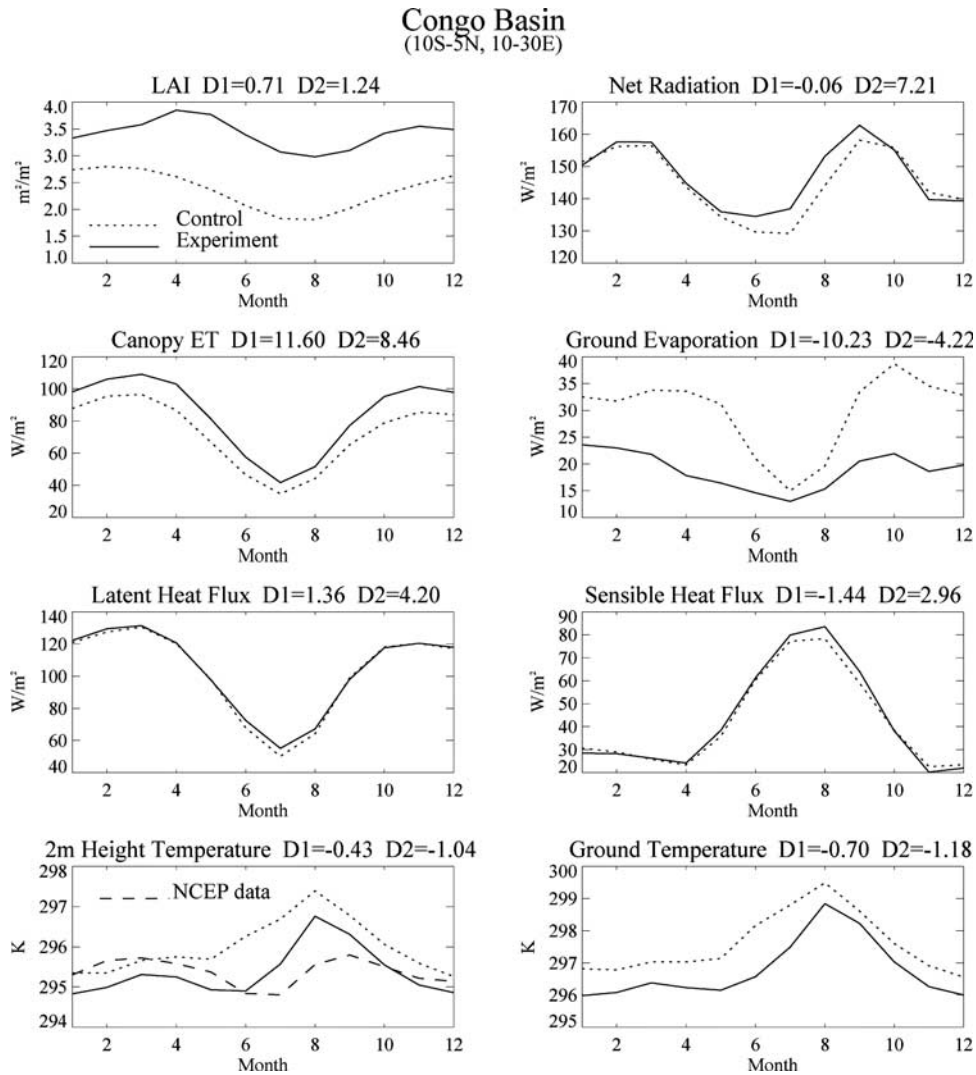

Figure 6. As in Figure 5 but for Congo Basin.

Tian et al., 2004b]. Consequently, albedo decreases significantly over the Amazon, central Africa, Alaska, eastern Siberia, and northern Europe in both winter and summer. More solar radiation absorbed by the surface because of the reduced albedo will modify energy balance between latent and sensible heat flux and thus will modify the local hydrological cycle (more discussion in section 4).

3.3. Differences in Surface Air Temperature

[15] Figures 4a and 4b show surface air temperature differences between the control run and the NCEP data. In winter a warm bias of several degrees is observed over high-latitude North America (>55°N), Middle East, and eastern Siberia while a cold bias is seen in the eastern United States and southeastern Asia. In summer, northern high latitudes are several degrees colder than the NCEP data, and a pronounced warming is seen over most northern middle latitudes. Amazon is warmer throughout the year, especially during the dry season. These biases are similar to those described by *Bonan et al.* [2002a], which compare the CLM2 temperature to observational data of C. J. Willmott and K. Matsuura (Terrestrial air temperature and precipitation: Monthly and annual climatologies, available at http://climate.geog.udel.edu/~climate).

[16] Figures 4e and 4f show the corresponding temperature differences between the experiment and control run. The new data generally lower the surface temperature in the tropics (15°S–10°N) during all seasons and thus reduce the warm bias over Amazon, Congo Basin, and Indonesia, especially in summer. They improve winter temperature simulations in eastern Siberia, Alaska, and northwest Canada and reduce the evident winter cold bias over the eastern United States and southeastern Asia. Note that the new land surface data degrade the simulation of surface air temperature over some regions, e.g., Congo and southeastern Brazil in wet season.

[17] The new data eliminate the summer cold bias beyond 50°N but generate a warm bias (Figure 4d) with a spatial pattern that is consistent with changes in the percent cover of snow (Figure 3d). As previously discussed, changes in the percent cover of snow are influenced by changes in land surface data and their triggered changes in solid precipitation (snow). Therefore the

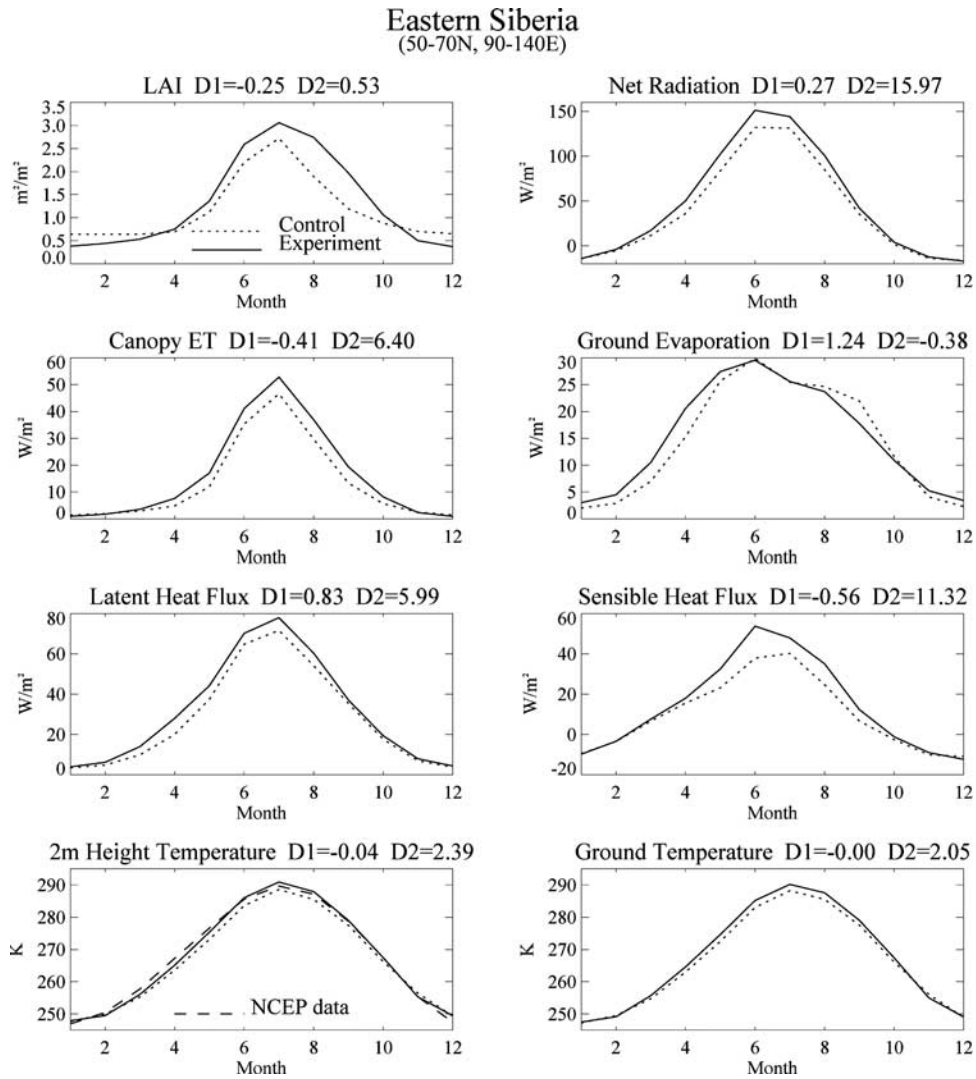

Figure 7. As in Figure 5 but for eastern Siberia.

significant temperature change in this region may result from both changes in the land surface data and the associated feedbacks.

4. Seasonal Variations at Regional Scales

4.1. Amazon (10°S–0°, 70°–50°W)

[18] In Amazon (Figure 5) the old LAI is smaller than the new one by as much as 1.6 during wet season but almost equals the new one in the dry season. The wet season LAI in the old data is too low relative to field measurements, which show that LAI is at least above 3.5 [*Honzak et al.*, 1996; *Roberts et al.*, 1996]. In addition, the expectation from vegetation phenology for this region is that LAI should remain constant with its value of dry season or peak during wet season. The seasonal cycle of the old LAI is out of phase with such expectation, possibly mainly due to data quality problems associated with AVHRR, such as lack of explicit atmospheric corrections and data contamination by extensive clouds during the wet season. The new LAI from MODIS collection 4 shows apparent improvements, consistent with the vegetation phenological expectation.

[19] The new LAI increases canopy evapotranspiration (ET) and decreases ground evaporation dramatically, especially during the wet season. Since little solar radiation and rainfall penetrate the dense tropical evergreen forests, evaporation from the ground should be ~10% of the total ET [*Arora and Boer*, 2002]. The higher LAI in the new data results in higher canopy conductance and energy exchange with the atmosphere by increasing the surface area from which moisture is lost and thus a relatively larger proportion of available energy for canopy ET [*Brutsaert*, 1982; *Bonan*, 2002] and less for ground evaporation.

[20] Part of the LAI increase is attributed to the change of ~20% of grass/crop into forest in the new data. Both the decrease in percent cover of grass/crop and the increase in LAI reduce surface albedo [*Tian et al.*, 2004b] and thus increase net radiation (absorbed solar radiation minus net longwave loss). As a result, latent heat flux (LE) increases by 3.21/4.58 W m^{-2} in the wet/dry season while sensible heat flux (H) shows a reduction or a small increase. Ground temperature drops by 0.8/1.3 K in response to the increased LE in wet/dry season, and air temperature declines by 0.6 K through the whole year. Similar results are seen in other

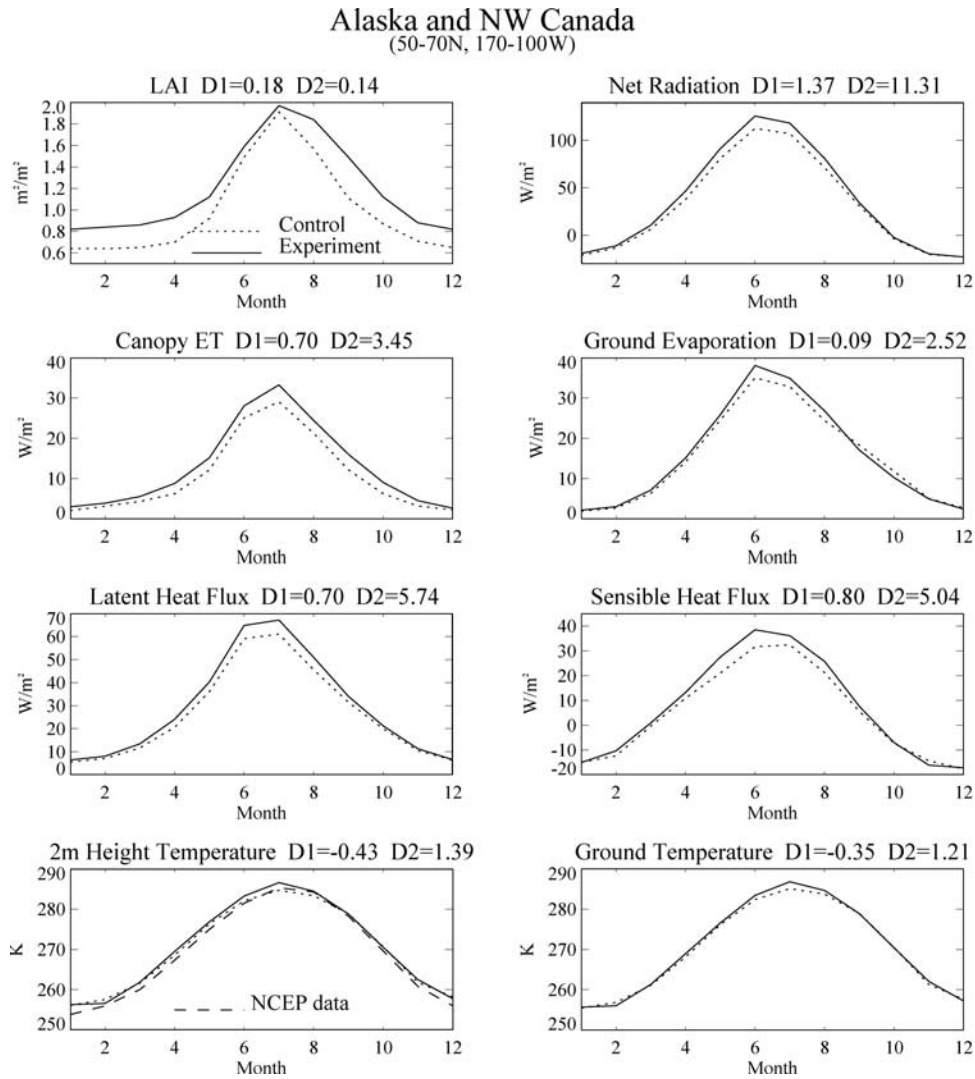

Figure 8. As in Figure 5 but for Alaska and northwestern Canada.

tropical regions (Figure 6) such as the Congo Basin (10°S–5°N, 10°–30°E), where the LAI is also underestimated in the old data.

[21] Vegetation parameters other than LAI could also, in part, have a contribution to the aforementioned changes. For example, when the land cover type is changed from grass/crop to forest, the roots of trees could access water in deep soil layers that are unavailable to those of grass/crop; this combined with the increased roughness length has the potential to increase canopy evapotranspiration and thus decreases temperature.

4.2. Eastern Siberia (50°–70°N, 90°–140°E)

[22] In this region the new data decrease the percent cover of grass/crop and replace it mostly with forest and shrub. During summer the new LAI is larger by 0.5 ~ 1 than the old data (Figure 7). The increases in LAI, percent cover of forest/shrub, and reduced solid precipitation decrease f_{sn} and thus lower albedo. Hence the net radiation increases by ~16 W m^{-2}, of which ~11 W m^{-2} is used for H, and the rest is used for LE. The larger increase in H than LE raises ground temperature by ~2 K and air temperature by ~2.4 K. Canopy ET also increases, while ground evaporation varies little. Similar results are observed in western Siberia and the region of Alaska and northwest Canada (e.g., Figure 8). Consequently, air temperature increases significantly in northern high latitudes (>50°N). During winter, changes in LAI have little effect on surface energy balance owing to cover of the vegetation by snow and lack of solar radiation. Rather, winter temperatures are largely determined by large-scale storm systems and cloud cover that may be of oceanic origin and are little affected by the surface.

4.3. Southeastern China (20°–30°N, 105°–120°E)

[23] Surface air temperature in this region increases/decreases during winter/summer in the experiment compared to the control run (Figure 9). In winter, f_{sn} decreases because of the LAI increase, which, in turn, increases the net radiation (mainly because of more solar absorption) and thus H (5.33 W m^{-2}). As a result, surface temperature increases. During summer the larger LAI and the replacement of grass/crop by tree in the new data result in more solar energy absorbed by vegetation and thus an increase in the net radiation. Because of the abundant precipitation in

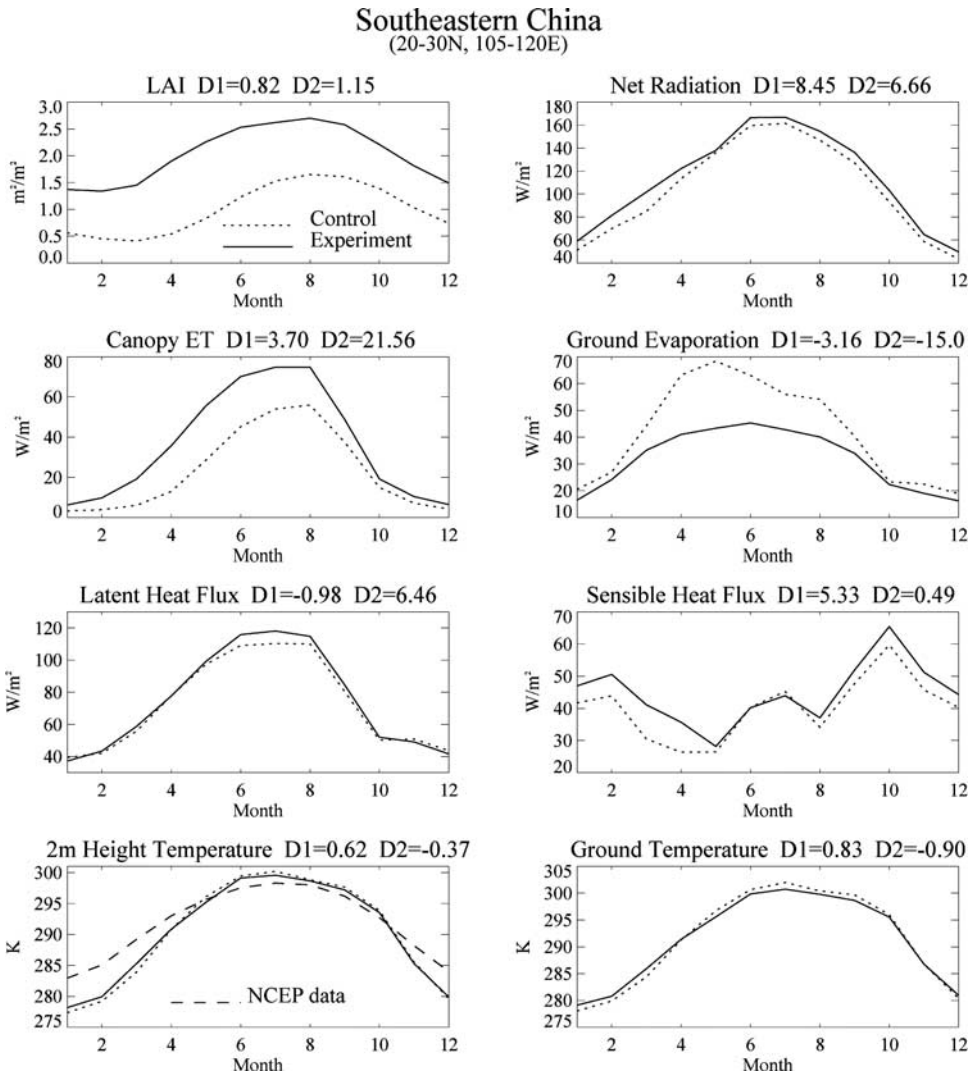

Figure 9. As in Figure 5 but for southeastern China.

this region (summer monsoon) and because of more trees most of the increased net radiation is converted to LE (6.46 W m^{-2}) for enhanced canopy ET. As a positive feedback, precipitation increases during summer (figure not shown) and thus reduces the drought in the control run [*Bonan et al.*, 2002a], and the surface air temperature is slightly colder. These changes in summer are similar to those over the Amazon region.

4.4. Eastern United States (30°–50°N, 90°–70°W)

[24] In the eastern United States (Figure 10), surface air temperature increases in both winter and summer compared to the control run. During winter the increased LAI and reduced snow decrease f_{sn} and thus warm the land surface. During summer the new LAI decreases by 1 and thus increases net radiation a little, which increases surface temperature, as most of it is used for increasing H. However, this warming enhances the positive temperature bias. Similar results are observed in central Europe (40°–55°N, 10°W–40°E). The reduced LAI in summer over these two regions may result from the relatively higher LAI for crops in the AVHRR data set compared with the MODIS data.

[25] However, the simulation of surface air temperature over southeast Brazil during wet season is degraded possibly because some forests are replaced by grass/crop and shrub in the new data, which leads to lower LAI and roughness length and shallower root depth. These changes result in reduced evapotranspiration and thus lead to warmer temperature.

5. Discussion and Conclusions

[26] This paper has examined how the land surface climate variables in CLM2 are improved by using a new land surface data set created from high-quality MODIS data of LAI, PFT, and FVC that is created from the MODIS vegetation continuous fields [*Tian et al.*, 2004b]. The old surface data in CLM2 underestimate LAI and overestimate the percent cover of grass/crop globally over most areas compared to the new data. Results indicate that changes in LAI and percent cover of grass/crop, tree, shrub, and bare soil substantially modify the surface fluxes, resulting in improved simulation of surface temperature in CLM2.

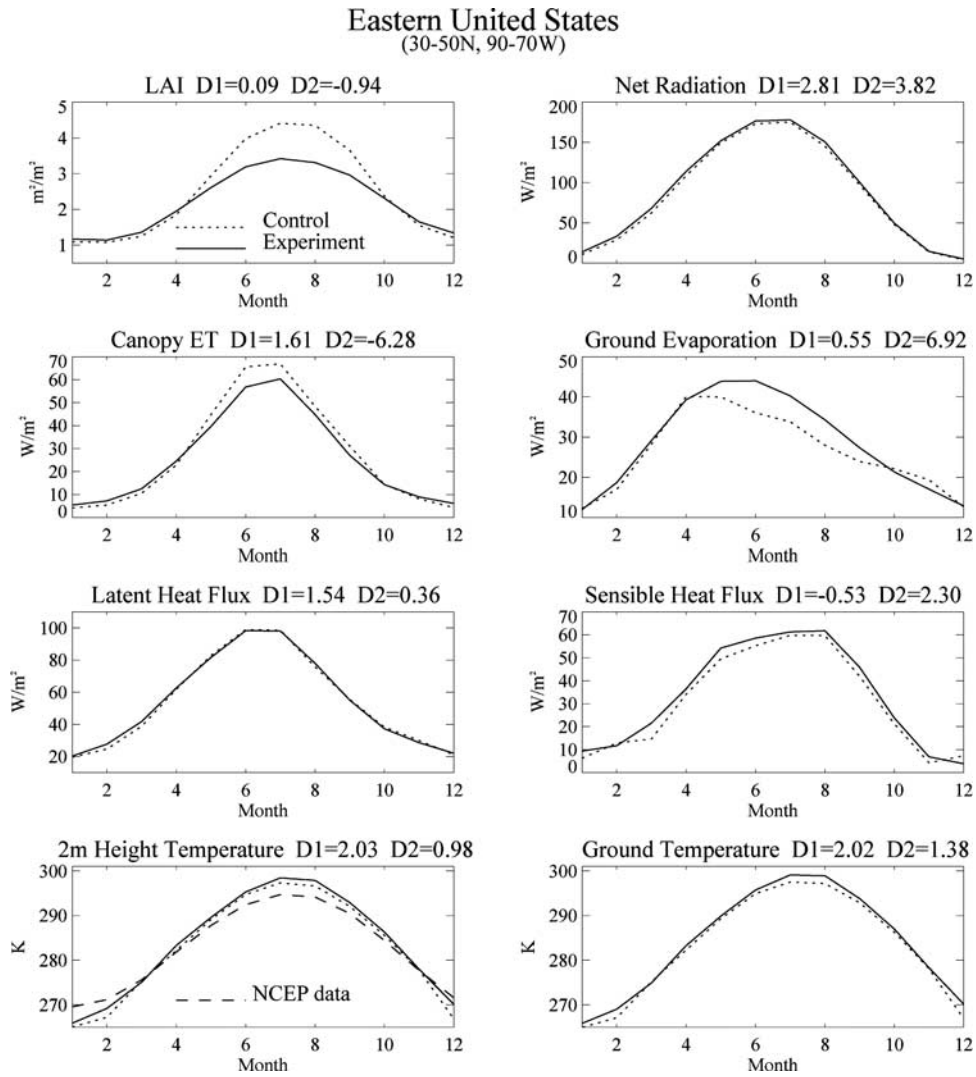

Figure 10. As in Figure 5 but for the eastern United States.

[27] The new data set largely decreases ground evaporation and increases canopy ET over tropical forests such as Amazon, Congo Basin, and Indonesia, especially during the wet season. With the improved quality of LAI and percent cover of tree from MODIS relative to AVHRR these changes move these two variables closer to reality. The new data set also reduces the model warm biases in these regions.

[28] The new data set also improves surface air temperature in northern middle and high latitudes, with more in summer than in winter. For snow-covered areas with abundant solar energy, changes in surface temperature largely depend on those in LAI and percent cover of tree/shrub. The higher LAI and more trees or shrubs in the new data set decrease the percent cover of snow, increase absorbed solar radiation and net radiation, and therefore raise ground and surface air temperature, which reduces the cold bias in CLM2. Over snow-free regions the increases in LAI and percent cover of tree from grass/crop increase latent fluxes and decrease surface air temperature.

[29] Surface air temperature biases still remain over some regions, however, presumably from other factors not addressed here. For regions where the effects of changes cancel out (such as a decrease in the percent cover of grass/crop and an increase in the percent cover of bare soil) the net changes can be very small and depend on which effect dominates. In particular, the surface air temperature over semiarid regions does not improve much, although the percent cover of bare soil is more reasonable in the new data set. The summer warm biases over the southeastern United States and central Europe are enhanced because of decreased LAI. Winter temperatures change little in regions that are fully covered by snow (e.g., Eurasia) and have limited solar energy.

[30] In summary, the use of the new land surface data improves the absorption and partitioning of energy between canopy and soil and, in doing so, provides more realistic surface air temperatures in CLM2, especially over the vegetated areas. The need for an accurate specification of land surface parameters, especially LAI, PFT, and FVC, is thus demonstrated.

[31] **Acknowledgments.** This work is funded by NASA grants NNG04GK87G and NNG04GO61G. We especially thank K. W. Oleson and S. Levis from NCAR for their assistance in processing the land surface data sets. NCEP reanalysis data provided by the NOAA-CIRES Climate Diagnostics Center in Boulder, Colorado, United States, were downloaded

from http://www.cdc.noaa.gov/. We are grateful to reviewers for their constructive suggestions that have improved this manuscript significantly.

References

Arora, V. K., and G. J. Boer (2002), A GCM-based assessment of the global moisture budget and the role of land-surface moisture reservoirs in processing precipitation, *Clim. Dyn.*, *20*, 13–29.

Blackmon, M., et al. (2001), The Community Climate System Model, *Bull. Am. Meteorol. Soc.*, *82*, 2357–2376.

Bonan, G. B. (1996), A Land Surface Model (LSM version 1.0) for ecological, hydrological, and atmospheric studies: Technical description user's guide, *NCAR Tech. Note NCAR/TN-417+STR*, 150 pp., Natl. Cent. for Atmos. Res., Boulder, Colo.

Bonan, G. B. (1997), Effects of land use on the climate of the United States, *Clim. Change*, *37*, 449–486.

Bonan, G. B. (1998), The land surface climatology of the NCAR Land Surface Model (LSM 1.0) coupled to the NCAR Community Climate Model (CCM3), *J. Clim.*, *11*, 1307–1326.

Bonan, G. B. (2002), *Ecological Climatology, Concepts and Applications*, Cambridge Univ. Press, New York.

Bonan, G. B., K. W. Oleson, M. Vertenstein, S. Levis, X. Zeng, Y. Dai, R. E. Dickinson, and Z.-L. Yang (2002a), The land surface climatology of the NCAR Community Land Model coupled to the NCAR Community Climate Model, *J. Clim.*, *15*, 3123–3149.

Bonan, G. B., S. Levis, L. Kergoat, and K. W. Oleson (2002b), Landscapes as patches of plant functional types: An integrating concept for climate and ecosystem models, *Global Biogeochem. Cycles*, *16*(2), 1021, doi:10.1029/2000GB001360.

Brutsaert, W. (1982), *Evaporation Into the Atmosphere: Theory, History and Applications*, 299 pp., D. Reidel, Norwell, Mass.

Buermann, W., J. Dong, X. Zeng, R. B. Myneni, and R. E. Dickinson (2001), Evaluation of the utility of satellite-based vegetation leaf area index data for climate simulations, *J. Clim.*, *14*, 3536–3551.

Chase, T. N., R. A. Pielke, T. G. F. Kittel, R. Nemani, and S. W. Running (1996), Sensitivity of a general circulation model to global changes in leaf area index, *J. Geophys. Res.*, *101*, 7393–7408.

DeFries, R. S., et al. (1999), Continuous fields of vegetation characteristics at the global scale at 1-km resolution, *J. Geophys. Res.*, *104*, 16,911–16,923.

Friedl, M. A., et al. (2002), Global land cover mapping from MODIS: Algorithms and early results, *Remote Sens. Environ.*, *83*, 287–302.

Gutman, G. (1999), On the use of long-term global data of land reflectances and vegetation indices derived from the advanced very high resolution radiometer, *J. Geophys. Res.*, *104*, 6241–6255.

Hansen, M., R. DeFries, J. R. G. Townshend, R. Sohlberg, C. Dimiceli, and M. Carrol (2002), Towards an operational MODIS continuous field of percent tree cover algorithm: Examples using AVHRR and MODIS, *Remote Sens. Environ.*, *83*, 303–319.

Honzak, M., R. M. Lucas, I. do Amaral, P. J. Curran, G. M. Foody, and S. Amaral (1996), Estimation of the leaf area index and total biomass of tropical regenerating forests: Comparison of methodologies, in *Amazon Deforestation and Climate*, pp. 365–381, John Wiley, Hoboken, N. J.

Kalnay, E., et al. (1996), The NCEP/NCAR 40-year reanalysis project, *Bull. Am. Meteorol. Soc.*, *77*, 437–471.

Kistler, R., et al. (2001), The NCEP-NCAR 50-year reanalysis: Monthly means CD-ROM and documentation, *Bull. Am. Meteorol. Soc.*, *82*, 247–267.

Lu, L., and W. J. Shuttleworth (2002), Incorporation of NDVI-derived LAI into the climate version of RAMS and its impact on regional climate, *J. Hydrometeorol.*, *3*, 347–362.

Myneni, R. B., et al. (2002), Global products of vegetation leaf area and fraction absorbed PAR from year one of MODIS data, *Remote Sens. Environ.*, *83*, 214–231.

Oleson, K. W., and G. B. Bonan (2000), The effects of remotely sensed plant functional type and leaf area index on simulations of boreal forest surface fluxes by the NCAR Land Surface Model, *J. Hydrometeorol.*, *1*, 431–446.

Oleson, K. W., W. J. Emery, and J. A. Maskanik (2000), Evaluation of land surface parameters in the biosphere-atmosphere transfer scheme using remotely sensed data sets, *J. Geophys. Res.*, *105*, 7275–7293.

Oleson, K. W., G. B. Bonan, C. B. Schaaf, F. Gao, Y. Jin, and A. Strahler (2003), Assessment of global climate model land surface albedo using MODIS data, *Geophys. Res. Lett.*, *30*(8), 1443, doi:10.1029/2002GL016749.

Roberts, J. M., O. M. R. Cabral, J. P. da Costa, A.-L. C. McWilliam, and T. D. de A. Sá (1996), An overview of the leaf area index and physiological measurement during ABRACOS, in *Amazon Deforestation and Climate*, pp. 287–306, John Wiley, Hoboken, N. J.

Tian, Y., et al. (2004a), Comparison of seasonal and spatial variations of leaf area index and fraction of absorbed photosynthetically active radiation from Moderate Resolution Imaging Spectroradiometer (MODIS) and Common Land Model, *J. Geophys. Res.*, *109*, D01103, doi:10.1029/2003JD003777.

Tian, Y., R. E. Dickinson, L. Zhou, R. B. Myneni, M. Friedl, C. B. Schaaf, M. Carroll, and F. Gao (2004b), Land boundary conditions from MODIS data and consequences for the albedo of a climate model, *Geophys. Res. Lett.*, *31*, L05504, doi:10.1029/2003GL019104.

Xue, Y., M. J. Fennessy, and P. J. Sellers (1996), Impact of vegetation properties on U.S. summer weather prediction, *J. Geophys. Res.*, *101*, 7419–7430.

Zeng, X., R. E. Dickinson, A. Walker, M. Shaikh, R. S. DeFries, and J. Qi (2000), Derivation and evaluation of global 1-km fractional vegetation cover data for land modeling, *J. Appl. Meteorol.*, *39*, 826–839.

Zeng, X., M. Shaikh, Y. Dai, R. E. Dickinson, and R. B. Myneni (2002), Coupling of the Common Land Model to the NCAR Community Climate Model, *J. Clim.*, *14*, 1832–1854.

Zhao, M., A. J. Pitman, and T. Chase (2001), The impact of land cover change on the atmospheric circulation, *Clim. Dyn.*, *17*, 467–477.

Zhou, L., et al. (2003a), Comparison of seasonal and spatial variations of albedos from Moderate Resolution Imaging Spectroradiometer (MODIS) and Common Land Model, *J. Geophys. Res.*, *108*(D15), 4488, doi:10.1029/2002JD003326.

Zhou, L., R. E. Dickinson, Y. Tian, M. Jin, K. Ogawa, H. Yu, and T. Schmugge (2003b), A sensitivity study of climate and energy balance simulations with use of satellite-derived emissivity data over Northern Africa and the Arabian Peninsula, *J. Geophys. Res.*, *108*(D24), 4795, doi:10.1029/2003JD004083.

R. E. Dickinson, M. Shaikh, Y. Tian, and L. Zhou, School of Earth and Atmospheric Sciences, 311 Ferst Drive, Georgia Institute of Technology, Atlanta, GA 30332, USA. (ytian@eas.gatech.edu)